SANS from Poly(ethylene oxide)/Water Systems

B. Hammouda,* D. Ho, and S. Kline

Center for Neutron Research, National Institute of Standards and Technology, 100 Bureau Drive, Stop 8562, Building 235, E151, Gaithersburg, Maryland 20899-8562

Received September 21, 2001; Revised Manuscript Received August 20, 2002

ABSTRACT: The poly(ethylene oxide) (PEO)/water system is investigated using small-angle neutron scattering (SANS). This system associates to form hydrogen-bonded clusters at high enough concentrations. Two correlation lengths are observed: one long range representing cluster sizes and the other short range representing polymer chain correlations. Clusters are formed at a volume fraction of 4% hPEO in D_2O. An LCST transition is obtained between a mixed phase (through hydrogen bonding) and a demixed two-phase region. Solvent deuteration is seen to enhance hydrogen bonding. Deuteration of the polymer backbone is seen to enhance hydrophobic interactions. The average polymer contrast match method fails due to the isotopic dependence of specific interactions. Pressure was seen to lower the LCST by breaking hydrogen bonds. At even higher temperature (beyond the boiling point of water) a UCST transition was observed.

Introduction and Literature Review

There has been a great deal of research interest in poly(ethylene oxide) (PEO)/water systems. This interest stems from PEO's ability to adsorb on surfaces and at interfaces and its strong cluster formation characteristic. Its use is found in drag reducers, pharmaceuticals, and environmental cleanup agents among others. The similarity of its specific interactions (hydrogen-bonding and hydrophobic interactions) to those found in proteins and other biological materials makes PEO/water a useful simple enough model system to study biomolecular interactions. Hydrogen bonding plays an important role in the stabilization of proteins, and hydrophobic interactions play an important role in protein folding and stability.

PEO/water solutions have been the subject of a number of investigations using many analytical techniques.[1] Polymer clusters form above a critical concentration. Temperature tends to dissolve these clusters, yielding a homogeneous polymer solution. Hydrogen bonding is the driving force behind cluster formation. Light scattering measurements gave cluster sizes of the order of a micrometer. Sample filtration was observed to disturb (dissolve) the clusters, which then re-form with a kinetics time scale of the order of hours to days.[1]

The purpose of the research effort reported here is to investigate isotope effects on hydrogen bonding using small-angle neutron scattering (SANS), i.e., find out whether deuterium bonding is stronger than hydrogen bonding. Other authors have addressed this question using other systems and other measurement techniques. Wave absorption spectroscopy and molecular beam Fourier transform microwave spectroscopy have been applied to gas jets of ethylene oxide (EO)/water mixtures. The spectrum of the EO···DOH (D-bonding) interaction was found to be stronger than that of the EO···HOD (H-bonding) interaction. This is due to the lower EO···DOH zero-point vibrational energy because of the shrinking of the OH water bond upon deuteration.[2] Also, protein-folding dynamics depend on the exchange rate of H-bonded atoms in the hydration layer. Studies have shown that the D-bonded form of water is more stable than the H-bonded complex[3] in the hydration layer.

Another goal of this research is to investigate the effect of hydrostatic pressure on hydrogen bonding in PEO/water systems. Rheological studies showed that pressure lowers the phase separation temperature in PEO/water systems.[4] This points to the evidence that the tetrahedral structure of water is disturbed by pressure increase. The same conclusion (lowering of the phase transition temperature with pressure) has also been observed using static light scattering.[5]

After describing the experimental methods and conditions used, a number of specific investigations will be described. These are all related to the PEO/water system. Varying polymer concentration and temperature changes hydrogen bonding and therefore cluster structure as observed by SANS. Cases corresponding to deuteration of the water molecules, deuteration of the polymer backbone, and deuteration of both will be included. The neutron contrast match method is used in order to isolate single-chain structure. Finally, the effect of pressure on clusters and phase separation thermodynamics will be described.

Samples and Measurement Methods

The SANS technique along with the partial deuteration method has been used in order to investigate cluster morphology and phase transitions. The NIST NG3-SANS instrument was used in the following configuration: 6 Å neutron wavelength, sample-to-detector distances of 13 and 1.3 m in order to cover a wide momentum transfer range ($0.004\ Å^{-1} < Q < 0.5\ Å^{-1}$). Measurement times varied from 5 to 30 min depending on neutron contrast and polymer concentration. Temperature was varied from 10 to 90 °C in 20 °C increments for most samples. One sample (10% volume fraction $hPEO/D_2O$) was taken all the way to 170 °C inside a pressure cell. Overhead runs (empty cell and blocked beam) were also measured and subtracted from the scattering data. Direct beam transmission runs were used to scale the averaged data to an absolute cross section form (units of cm^{-1}). Gellike and solution samples were measured inside tightly sealed demount-

10.1021/ma011657n CCC: $22.00
Published on Web 09/25/2002

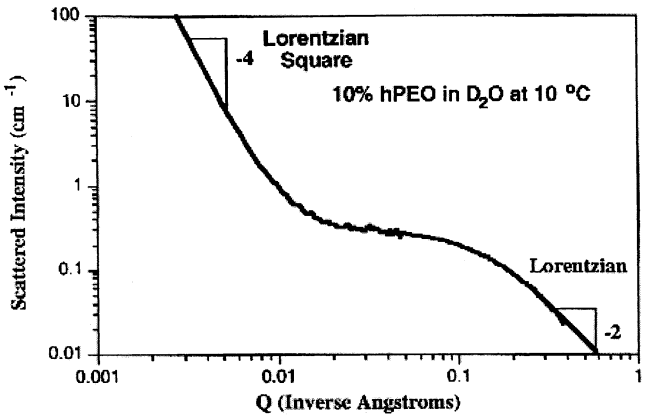

Figure 1. The two-correlation-length model. The low-Q mode ($\sim 1/Q^4$) characterizes the clusters (Lorentzian square), and the high-Q mode ($\sim 1/Q^2$) characterizes polymer chain correlations.

able cells with either 1 or 2 mm neutron path depending on whether H_2O or D_2O was used as solvent. A few samples were measured inside an in-situ pressure cell.

The pressure cell that was used for some of the measurements is the second generation of its kind at NIST. It can reach 3 kbar and allows measurements from below room temperature (10 °C for example) all the way to above the boiling point of water (100 °C) provided that a positive pressure differential (3 MPa is used here) is always kept on the sample in order to avoid boiling.

Because the measured samples had varying concentration (and therefore varying hydrogen amounts), no "pure incoherent scattering samples" (also referred to as buffer samples) were measured. Such samples would have consisted of mixtures of H_2O/D_2O in which the hydrogen number density would have matched that of the real PEO/water samples. Instead, the level of SANS incoherent background (Q-independent) was estimated from Kratky plots ($Q^2I(Q) = A + BQ^2$) at high Q from the constant value B. The high Q range ($0.2\ \text{Å}^{-1} < Q < 0.4\ \text{Å}^{-1}$) where the Kratky plot shows a linear variation was used.

The PEO polymers used were purchased from Polymer Source (Quebec, Canada), who also performed size exclusion chromatography (SEC) and gel permeation chromatography (GPC) to determine the molecular mass. For the hydrogenated PEO (hPEO), $M_w = 100\ 000$ and $M_n = 96\ 000$ and for the deuterated PEO (dPEO), $M_w = 102\ 000$ and $M_n = 97\ 700$, yielding a polydispersity index of 1.04 in both cases. Deuterated water (D_2O) was purchased from Cambridge Isotopes (>99%). Deionized water (H_2O) was used with no further treatment.

Samples for SANS measurements were usually prepared at least 1 day in advance and left to equilibrate. No filtration was performed, and no special time-dependent kinetics was observed. Some temperature scans (raising temperature) were repeated through a cooling cycle. No irreversible behavior was observed. Measurements from a few samples were repeated with fresh samples and at different times to test reproducibility. Within our experimental measurement conditions, no aging of the samples was observed.

The Two-Correlation-Length Model

Figure 1 shows SANS data from a typical PEO/water sample. The cluster feature at low Q and the typical Gaussian chain scattering at high Q are the dominant features. Following other SANS investigations of similar structures,[6,7] a simple, two-correlation-length model was used. The scattered intensity was fitted to the following functional form:

$$d\Sigma(Q)/d\Omega = A_1/(1 + Q^2R_1^2)^2 + A_2/(1 + Q^2R_2^2) \qquad R_1 > R_2 \quad (1)$$

The first term is used to describe the low-Q, long-range behavior ($\sim 1/Q^4$). The second term is the familiar Lorentzian function used to describe the high-Q, short-range behavior ($\sim 1/Q^2$). A_1 and A_2 are the relative weighting coefficients, and R_1 and R_2 are the long-range and short-range correlation lengths, respectively. This cross section describes the coherent scattering signal only. In practice, the scattered intensity also contains a constant (incoherent scattering) background B that is left as a floating parameter in fits to the above model. Values of B obtained from Kratky plots or from this method agree well.

The SANS technique did not allow us to observe the saturation downturn at low Q. The log(I) vs Q Porod plot remained linear all the way to low Q. Even a measurement on another neutron scattering instrument (the Bonze-Hart Ultra-SANS spectrometer) that can reach $Q_{min} = 0.000\ 06\ \text{Å}^{-1}$ still showed only a consistent log(I) vs log(Q) linear behavior. This is due to the fact that association clusters in the samples are huge (micron size). Clusters are represented by the low-Q mode (Lorentzian square). The SANS method is observing only the tail of these large-scale structures. Because no linear Guinier region was observed at low Q, radii of gyration could not be reliably estimated. Instead, we focused on the two correlation lengths R_1 and R_2. R_1 represents cluster sizes, and R_2 represents local correlations through polymer chain.

Varying Polymer Concentration

PEO is soluble in water. This is due to its hydrophilic interaction with water. The PEO molecule ($-CH_2-CH_2O-$) is characterized by the dual interplay of hydrophobic interactions (through the $-CH_2-\cdots HOH$ repulsive interaction) and hydrophilic hydrogen-bonding interactions (through the backbone $-CH_2O\cdots HOH$ attractive interaction). For low temperatures, and above a critical polymer concentration, the hydrogen-bonding interactions are dominant, and PEO is not only soluble in water but also forms H-bonded clusters through physical cross-linking of the PEO macromolecules with themselves. This cross-linking is mediated by water molecules through the $CH_2CH_2O\cdots HOH\cdots OCH_2CH_2$ interactions. The CH_2 groups cannot hydrogen bond; only the backbone oxygens can.

In these measurements, we prepared a series of $hPEO/D_2O$ samples where polymer concentration was varied. Figure 2 shows the SANS data at 10 °C. As the concentration increases, the low-Q feature appears and becomes stronger pointing to the formation and growth of the clusters. Nonlinear least-squares fits to the described model gave two correlation lengths R_1 and R_2 that varied with opposite trends when the polymer concentration was increased. Whereas R_1 increased with concentration (clusters are getting bigger), R_2 decreased, implying that short-range correlations are getting shorter. Extrapolation of the data in Figure 3 leads to a merging of the two correlation lengths to a common value around 100 A. This common length is obtained for a polymer

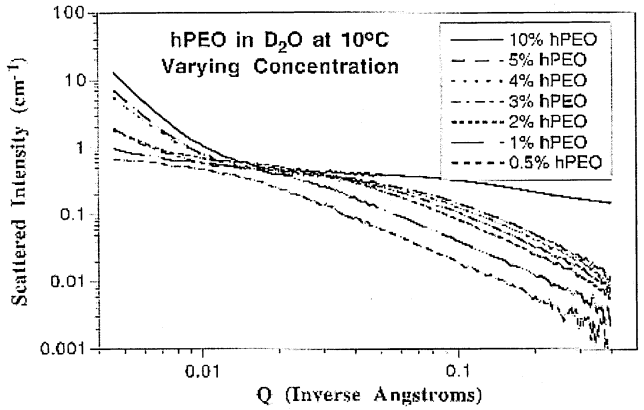

Figure 2. SANS from hPEO/D_2O for increasing polymer concentration (volume fraction) at 10 °C. As the concentration increases, the low-Q feature (characterizing clusters) appears and becomes stronger.

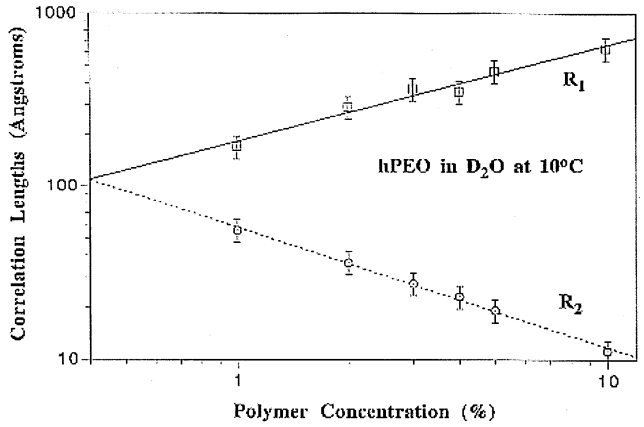

Figure 3. Variation of the two correlation lengths for the hPEO/D_2O system for increasing polymer concentration (volume fraction) and at 10 °C.

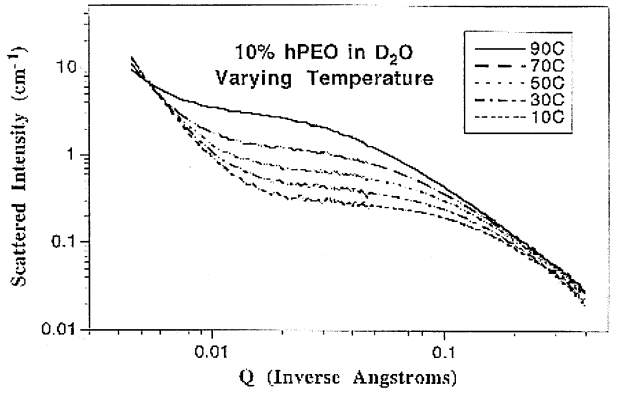

Figure 4. SANS from the 10% hPEO/D_2O sample for increasing temperature. As the temperature increases, the low-Q feature (clusters) becomes weaker and the high-Q feature becomes stronger.

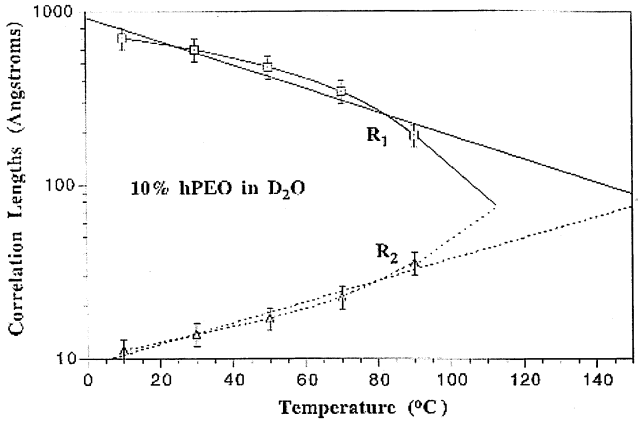

Figure 5. Variation of the two correlation lengths for the 10% hPEO/D_2O sample for increasing temperature.

volume fraction of 0.4% (associated with the cluster formation concentration). It represents the free polymer coil size in the completely dissolved state. It is interesting to observe that Figure 3 shows linear behaviors, implying power law dependencies upon polymer concentration for the two correlation lengths ($R_1 \sim c^{0.65}$ and $R_2 \sim c^{-0.545}$). The authors of this paper are unaware of any such predictions in the literature. In Figure 3, the error bars correspond to both statistical uncertainty and data fitting precision.

It should be noted that, for the polymer concentrations considered here, no sample crystallinity was observed by wide-angle X-ray scattering (WAXS).

Varying Temperature

It is well-known that heating breaks down hydrogen bonds. Increasing temperature for our hPEO/D_2O set of samples does not change the overall character of the scattering. The low-Q ($\sim 1/Q^4$) and the high-Q ($\sim 1/Q^2$) behaviors are conserved, but the range of the interactions and their relative strengths change (Figure 4). Breaking hydrogen bonds dissolves the clusters. Extrapolation of the R_1 and R_2 trends at high temperatures yields again one unique length scale comparable to the polymer coil size in solution (Figure 5). Figure 5 shows interpolation of the data along with an exponential fit (merely as a guide to the eyes). This fit is the closest feature available in Kaleidagraph but still does not follow the data closely. It is not implied, here, that the data should follow an exponential law.

An Incomplete Temperature/Concentration Phase Diagram

The coefficient A_2 represents the strength of the Lorentzian component of the two length-scale model. In the limit of no clusters, the random phase approximation (RPA) for polymer solutions gives the following cross section:

$$\text{contrast}/A_2 \sim (a_P/V_P - a_S/V_S)^2/d\Sigma_S(Q)/d\Omega = (N\phi_P V_P)^{-1} + (\phi_S V_S)^{-1} - 2X_{PS}/V_0 \quad (2)$$

where a_P, N, ϕ_P, and V_P are the scattering length, degree of polymerization, volume fraction, and specific volume for the polymer and a_S, ϕ_S, and V_S are the equivalent quantities for the solvent. X_{PS} is the usual Flory–Huggins interaction parameter, and V_0 is a "reference" volume. Solution thermodynamics are buried in X_{PS}. For instance, the spinodal temperature is obtained from the intercept in the plot $1/d\Sigma_S(Q)/d\Omega$ vs $1/T$ (K). In our hydrogen-bonded system, the scattering is very much different at low Q ($\sim 1/Q^4$), but the high-Q feature is expected to contain information about local chain thermodynamics. Of course, the Flory–Huggins parameter X_{PS} will include van der Waals as well as hydrogen-bonding and hydrophobic interaction contributions.[5] Without further attempts at justification (other than

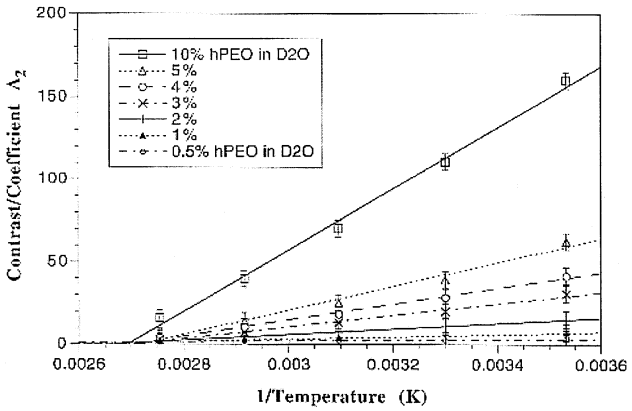

Figure 6. Variation of the A_2 coefficient (normalized by the neutron contrast) with temperature (in K) for the concentration series of hPEO/D_2O samples measured. The intercept of the A_2^{-1} vs T^{-1} plot is the extrapolated spinodal temperature. The term "contrast" is used, here, to denote the prefactor of $P_T(Q)$ in eq 3.

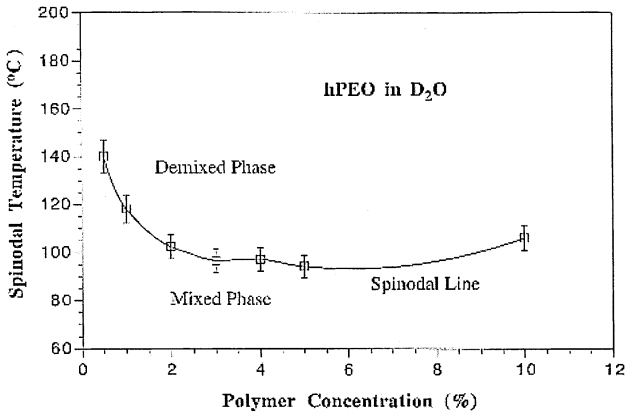

Figure 7. Part of the temperature/concentration phase diagram for the hPEO/D_2O system corresponding to the measured concentrations.

this method seems to work well), we plotted $1/A_2$ vs $1/T$ (K) in Figure 6 for the concentration series of the hPEO/D_2O samples measured. The behavior is linear, which means that the $1/T$ dependence of the Flory−Huggins X parameter holds even for these hydrogen-bonded systems. The intercept obtained for $1/A_2 = 0$ yields a spinodal temperature, which is reported in Figure 7. This figure constitutes the low-concentration end of the temperature/concentration phase diagram, showing a spinodal line that separates the demixed phase (high temperature) from the mixed phase (low temperature) in this lower critical solution temperature (LCST) system. We emphasize that this is a phase transition line between a hydrogen-bonded single-phase region and a two-phase region. The system mixes through hydrogen bonding and demixes when hydrogen bonding weakens.

So far, deuteration was included only in the solvent through the use of D_2O. In what follows, the great asset of the SANS technique, i.e., the average contrast match method, is used.

The Zero Average Contrast Match Method

To assess the effect of deuteration of the polymer backbone on hydrogen bonding, we prepared a series of PEO samples in D_2O. In this series, the total polymer concentration was kept constant (volume fraction of 4%), but the relative amount of dPEO/PEO was varied (referred to as series I in Figure 8). To isolate single-chain contributions for this series, we prepared another series (series II in Figure 8) where we used mixtures of D_2O and H_2O solvent molecules that contrast-match the average polymer scattering length density. For such hPEO/dPEO/H_2O/D_2O mixtures, the scattering intensity is given by

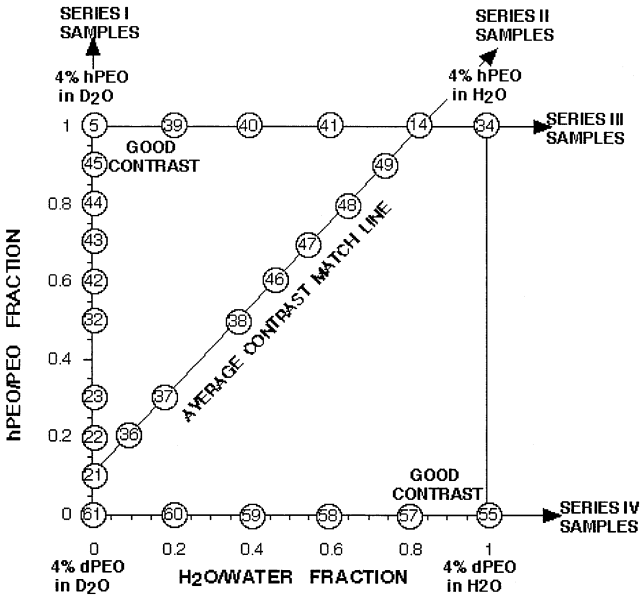

Figure 8. Summary of the samples measured by SANS (numbers inside circles are the sample numbers). For all these samples, the total polymer volume fraction was kept constant at 4%.

$$d\Sigma(Q)/d\Omega = (a_H/V_H - a_D/V_D)^2[\phi_H\phi_D/\phi_P^2]N_P\phi_PV_PP_S(Q) + [(a_D\phi_D/\phi_PV_P + a_H\phi_H/\phi_PV_P) - a_S/V_S]^2N_P\phi_PV_PP_T(Q) \quad (3)$$

Here, a_H and a_D are the scattering lengths for the hPEO and dPEO monomers, V_H and V_D are the corresponding specific volumes, and ϕ_H and ϕ_D are the corresponding polymer volume fractions (and similarly for the solvent scattering length density a_S/V_S). To arrive at this formula, it was assumed that the protonated and deuterated polymer degrees of polymerization and specific volumes are matched. The degree of polymerization used here, N_P, represents that for the two mixed polymer species ($N_H = N_D = N_P$). The total polymer volume fraction ϕ_P ($\phi_P = \phi_H + \phi_D$) and polymer specific volume V_P ($V_P = V_H = V_D$) have also been defined. So have the single-chain structure factor $P_S(Q)$ and the total chain structure factor (including intrachain and interchain contributions) $P_T(Q)$. The average contrast match condition zeroes the second term in eq 3, leaving only the first term proportional to $P_S(Q)$.

This formula (eq 3) assumes that deuteration does not affect chain structure or interactions. This is obviously a strong assumption for our hydrogen-bonded system.

Specific values for the defined parameters for our system are as follows: $N_{hPEO} = 2273$, $N_{dPEO} = 2125$, $a_{hPEO} = 4.14 \times 10^{-13}$ cm, $a_{dPEO} = 45.78 \times 10^{-13}$ cm, $a_{H_2O} = -1.67 \times 10^{-13}$ cm, $a_{D_2O} = 19.14 \times 10^{-13}$ cm, $V_{hPEO} = V_{dPEO} = 38.94$ cm^3/mol, and $V_{H_2O} = V_{D_2O} = 18$ cm^3/mol. The four possible contrast factors corresponding to the four corners in Figure 8 are as follows:

$$(a_{dPEO}/V_{dPEO} - a_{H2O}/V_{H2O})^2A = 9.657 \times 10^{-3} \text{ mol/cm}^4$$

$$(a_{\mathrm{hPEO}}/V_{\mathrm{hPEO}} - a_{\mathrm{D_2O}}/V_{\mathrm{D_2O}})^2 A = 5.498 \times 10^{-3}\ \mathrm{mol/cm^4}$$

$$(a_{\mathrm{hPEO}}/V_{\mathrm{hPEO}} - a_{\mathrm{H_2O}}/V_{\mathrm{H_2O}})^2 A = 2.384 \times 10^{-4}\ \mathrm{mol/cm^4}$$

$$(a_{\mathrm{dPEO}}/V_{\mathrm{dPEO}} - a_{\mathrm{D_2O}}/V_{\mathrm{D_2O}})^2 A = 7.529 \times 10^{-5}\ \mathrm{mol/cm^4}$$

Here we have multiplied by Avogadro's number ($A = 6.022 \times 10^{23}$molecules/mol) for convenience. The strongest neutron contrasts correspond to the two mixtures: dPEO/H_2O and hPEO/D_2O. Contrasts corresponding to the other two mixtures are much lower.

Moving across from corner to corner in Figure 8 allows us to test isotope effects on both hydrogen-bonding and hydrophobic interactions. Because the backbone CH_2 groups are not supposed to participate in the hydrogen-bonding process, their deuteration (in the vertical series I samples) tests hydrophobic interactions. Because hydrogen bonding is mediated across polymer chains through water molecules, series III and IV samples (horizontal scans) test pure hydrogen bonding. Series II samples (almost diagonal scan) involve a mixture of both effects.

Varying the Deuterium Content in the Water

Moving along series IV samples allows us to test isotope effects on hydrogen bonding. Figure 9 depicts the variation of the A_1 coefficient (strength of the cluster mode) along this series. It can be seen that deuterated (heavy) water mediates stronger hydrogen bonding than normal (light) water. Deuterium bonding is much stronger than hydrogen bonding. This leads to more clustering as observed by SANS. It is surprising to see that the dPEO/D_2O (low contrast) sample scatters more than the dPEO/H_2O (high contrast) sample because of the stronger cluster inhomogeneities. The intermediate-Q plateau region is nonexistent for the dPEO/D_2O sample because of the poor contrast between polymer chains and solvent. This conclusion agrees with findings obtained using other analytical methods.[2,3]

Similar results were obtained for the series III samples. However, incoherent scattering from H_2O overwhelms the SANS signal close to the hPEO/H_2O corner and makes the SANS data flat and useless.

Varying the Deuterium Content in the Polymer Backbone

Series II samples correspond to the average contrast match condition whereby the second term in eq 3 is zero. For this series, mixtures of D_2O and H_2O are used to match the average contract for the dPEO/hPEO polymer mixtures. Subtracting the incoherent background and rescaling the SANS data by the prefactor of the first term in eq 3 gives the single-chain structure factor $P_S(Q)$, which is shown in Figure 10 for a few series II samples (at 10 °C). $P_S(Q)$ is supposed to be the same for all the measured samples. Figure 10 shows quite a bit of variation, especially at low Q, pointing to the breakdown of deuteration methods for hydrogen-bonded systems.

Series I samples test the effect of isotope substitution in the polymer backbone. Figure 11 shows SANS data for a few of these samples. Because these samples contain contributions from the first and second terms of eq 3 and because the first term has a quadratic variation of the neutron contrast on ϕ_{hPEO}, the hPEO volume fraction, these results are not very helpful trend monitors. It can be concluded, however, that the two corners of this series (volume fractions of 4% dPEO/D_2O and 4% hPEO/D_2O) show a low-Q ($\sim 1/Q^4$) feature clearly pointing to well-formed clusters. Moreover, the dPEO/D_2O sample has a larger value of R_1 (cluster sizes). The "A_1/contrast" coefficient varies from 1443 for sample 61 (dPEO/D_2O) to the low value of 3 for sample 5 (pure hPEO/D_2O). The term "contrast" is used, here, to denote the prefactor of $P_T(Q)$ in eq 3. Deuteration of the polymer backbone strengthens the clusters by enhancing the hydrophobic interaction.

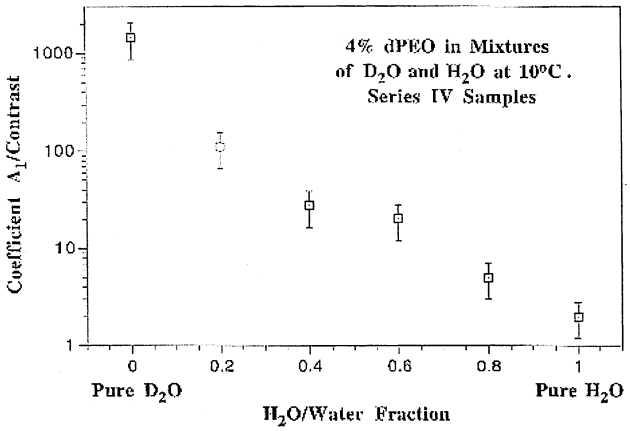

Figure 9. Variation of the A_1 coefficient (strength of the scattering from clusters) for the series IV samples where the relative amount of deuterium in the water is varied.

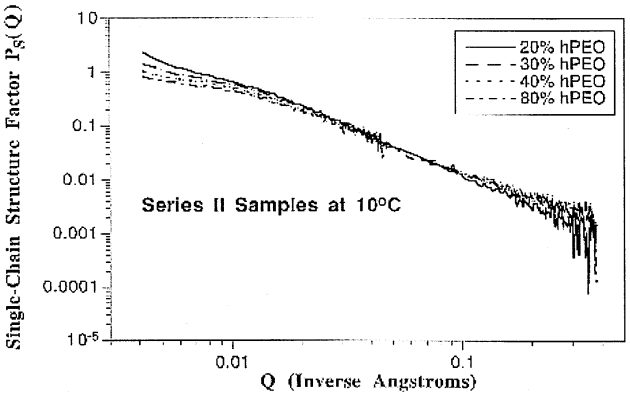

Figure 10. Variation of the single-chain structure factor $P_S(Q)$ for the series II samples at 10 °C. Note the low-Q discrepancies between the various curves indicating nonnegligible isotope effects (H-bond and D-bond are different).

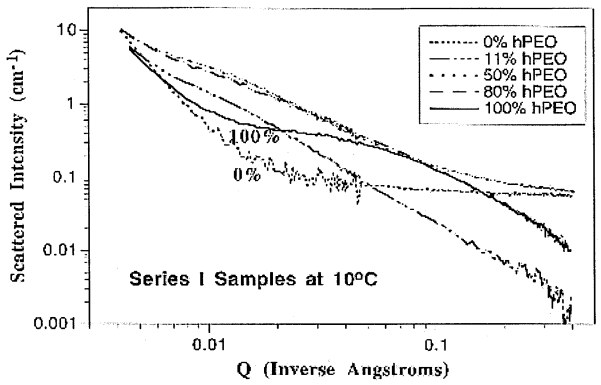

Figure 11. Variation of the SANS scattered intensity for the series I samples whereby various volume fractions of D replace H on the polymer backbone, keeping the total polymer volume fraction fixed at 4%.

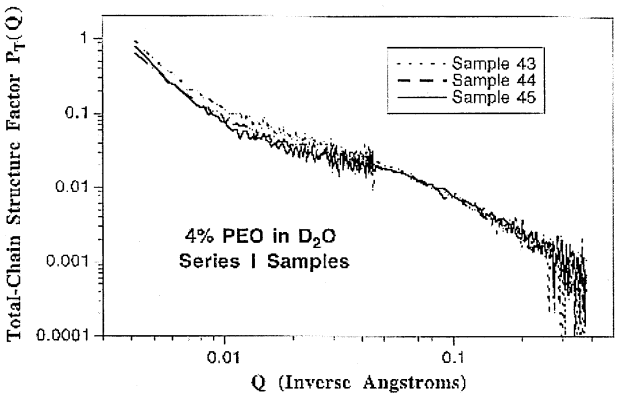

Figure 12. Total-chain structure factors $P_T(Q)$ obtained by combining data from series I and series II samples. If isotope effects were negligible, these curves would be identical.

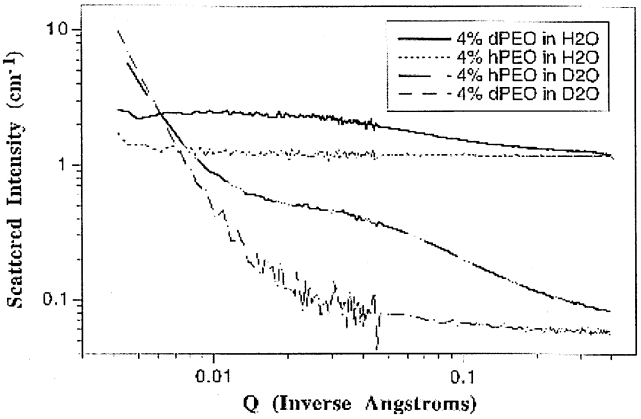

Figure 13. Comparison of the scattering curves obtained from the four samples corresponding to all possible deuteration schemes (hPEO/D_2O, hPEO/H_2O, dPEO/D_2O, and dPEO/H_2O). These correspond to the four corners in Figure 8. The two top curves contain H_2O (large incoherent background) that was not subtracted. The two bottom curves correspond to D_2O solvent instead.

SANS data from series II samples are subtracted from those of series I samples and rescaled in order to isolate the total-chain structure factor $P_T(Q)$ given in eq 3 as shown in Figure 12. It is reassuring to see that $P_T(Q)$ shows the low-Q ($\sim 1/Q^4$) mode as well as the high-Q ($\sim 1/Q^2$) mode as it should. Whereas $P_S(Q)$ has contributions mostly from polymer chains, $P_T(Q)$ has contributions from the clusters as well. We emphasize here again that if the deuteration method had worked well, all curves in Figure 12 would have fallen on top of each other. The deuteration method breaks down when used on systems containing hydrophobic interactions because it changes the strength of these interactions.

The Four Deuterium Label Swapping PEO/Water Pairs

The conclusions reached so far are as follows. Stronger clustering is obtained when water is deuterated and/or when the polymer backbone is deuterated. Because these are important conclusions, we would like to reinforce these findings. Summarizing in Figure 13 the SANS raw data (no background subtracted, no rescaling done) obtained for the four corners of Figure 8, we can rank cluster formation as follows. Strongest cluster formation is obtained for dPEO/D_2O, then for hPEO/D_2O, then for dPEO/H_2O, and then finally for hPEO/H_2O (weakest cluster formation). This conclusion is reached by pure observation of the raw data (low-Q feature) with no data treatment of any sort. Note that the high-Q behavior of the curves in Figure 13 flattens out (instead of the $\sim 1/Q^2$ behavior) because no incoherent background B was subtracted. The spinodal temperature for the 4% dPEO/D_2O sample was estimated to be around 140 °C whereas that for 4% hPEO/D_2O was estimated to be around 97 °C.

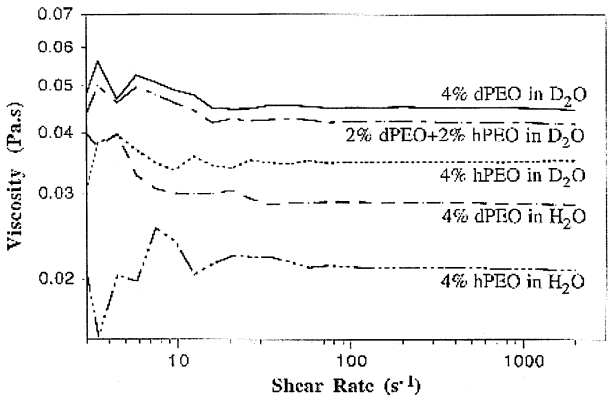

Figure 14. Comparison of the viscosity measurements from the four samples corresponding to all possible deuteration schemes (as in Figure 13).

Furthermore, we measured the viscosity of the four samples in question using a Couette-type rheometer. Rheology is a good monitor of cluster formation. Figure 14 shows that the same ranking in cluster formation observed by SANS holds with rheology. This figure also shows an intermediate case (corresponding to sample 32 in Figure 8) with 2% hPEO + 2% dPEO in D_2O. The viscosity of that sample is in between the two expected limits but lays closer to the lower limit (sample 61).

The same conclusions were reached for a series of four 10% (label swapping) PEO/water sample pairs.

Pressure Effects

Hydrostatic pressure has been previously applied to PEO/water systems.[4,5] These two investigations used different measurement methods (rheology and light scattering) to conclude that pressure lowers the phase separation line due to pressure-induced breaking of hydrogen bonds. We measured two samples containing volume fractions of 4% and 10% hPEO/D_2O by SANS under wide pressure (3−267 MPa) and temperature (10−90 °C) conditions. The 10% hPEO/D_2O sample was measured under an even wider temperature range (10−170 °C). This necessitated the use of another heating jacket for the pressure cell (heating cartridges instead of circulating bath).

Fits of the SANS data to the two-length scale model gave values for the A_2 coefficient that are used in Figure 15. As done previously, the intercept of the $1/A_2$ vs $1/T$ (K) plot gave estimates for spinodal temperatures. These LCST spinodal temperatures are seen to decrease with increasing pressure (Figure 16) by as much as 5 °C/kbar.

Moreover, the A_2 coefficient for the 10% hPEO/D_2O sample increases with temperature toward an LCST (estimated to be around 106 °C at 3 MPa), levels off, and then decreases at higher temperatures beyond a UCST (estimated to be around 115 °C at 3 MPa). This leaves a window (between 106 and 115 °C) where the sample can demix (immiscibility island). Figure 17 shows that hydrostatic pressure lowers both the LCST and the UCST.

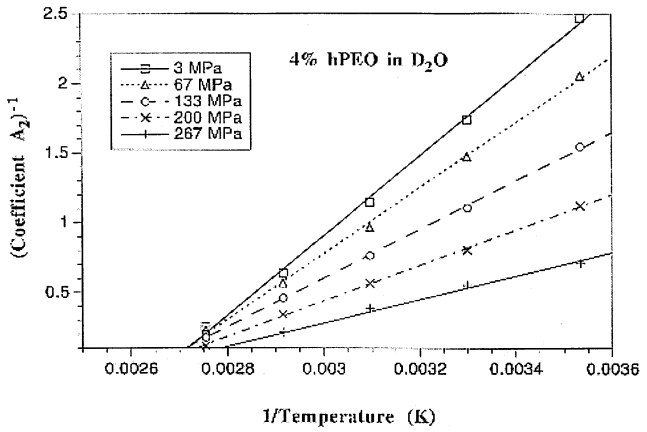

Figure 15. Variation of the A_2 coefficient (normalized by the neutron contrast) with temperature (in K) for increasing pressure on the 4% hPEO/D_2O sample. The intercept of the A_2^{-1} vs T^{-1} plot is the extrapolated spinodal temperature. The term "contrast" is used, here, to denote the prefactor of $P_T(Q)$ in eq 3.

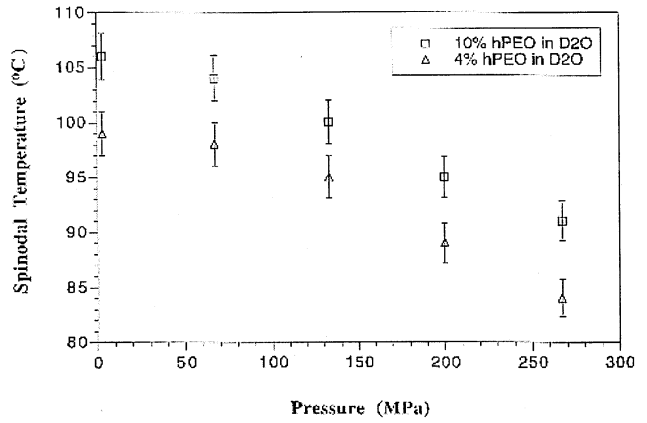

Figure 16. Pressure dependence of the spinodal temperature for two samples (4% hPEO/D_2O and 10% hPEO/D_2O).

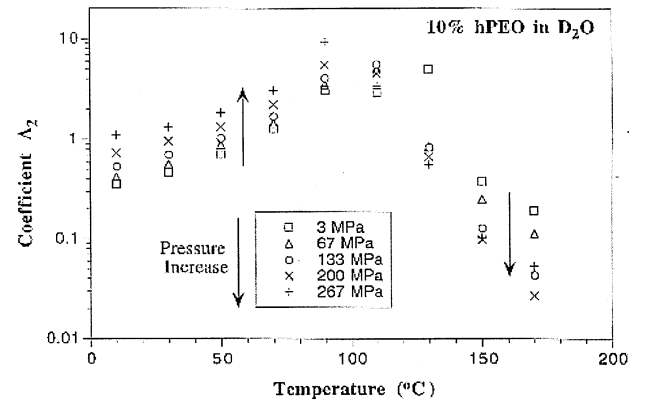

Figure 17. Variation of the coefficient A_2 characterizing the thermodynamic phase separation behavior of the 10% hPEO/D_2O.

An immiscibility island phase diagram behavior has been observed in C_4E_1 surfactant ($CH_3CH_2CH_2CH_2$-OCH_2CH_2OH) in water[8] and in other water-soluble polymers.[9] Note the chemical structure resemblance between C_4E_1 and the ethylene oxide monomer. Water-soluble polymers are held together by hydrogen bonding. At high temperatures, hydrogen bonding breaks down, allowing the system to demix and form a two-phase region. This region, however, ends at higher temperatures (UCST) where other interactions (hydrophobic, van der Waals) weaken, leading to a high-temperature one-phase region.

Summary of the Results

The PEO/water system was investigated using the SANS technique. This system forms hydrogen-bonded clusters at high enough concentrations. Two correlation lengths characterized the scattering: one long range representing cluster sizes and the other short range representing polymer chain correlations. The two correlation lengths were observed to merge to the polymer coil size below a critical cluster formation concentration and above a temperature for which hydrogen bonds weaken substantially. Power law variations between these correlation lengths and the polymer concentration were observed.

The prefactor, A_2, of the Lorentzian mode in the two-correlation-length model contains thermodynamic information about polymer chain miscibility. A plot of $1/A_2$ vs $1/T$ (K) gave estimates of the spinodal temperature for the LCST transition. Mapping of this spinodal temperature yielded the lower-left part of the temperature/concentration phase diagram.

Partial deuteration of the water solvent showed stronger D-bonding than H-bonding. Deuteration of the polymer backbone showed stronger hydrophobic interactions for deuterated polymer than for protonated (hydrogenated) polymers. Because of these isotope effects on specific interactions, the conventional deuteration technique fails.

Pressure was seen to lower the LCST by breaking hydrogen bonds. This lead to a demixing phase transition from the mixed one-phase (through hydrogen bonding) to a demixed two-phase region. Increasing temperature beyond the boiling point of water showed a UCST phase transition leading to another, high-temperature, mixed-phase region.

The overall scenario coming out of these investigations comprises two main driving forces: hydrogen bonding and hydrophobic interactions. Hydrogen-bonding ($CH_2O\cdots HOH\cdots OCH_2$) interactions form physical bonds between oxygen atoms and therefore between monomers. Moreover, $OCH_2\cdots HOH$ hydrophobic interactions tend to repel water molecules and favor $CH_2\cdots CH_2$ polymer−polymer attractive interactions.

The PEO/water system may be the simplest model to study biomolecular interactions; it certainly is a complex puzzle to sort out. Our efforts reported here as well as those of others before us are starting to give us a faint glimpse at what is really happening. The picture is far from complete.

Final Note

After having completed this research, ref 10 came to our attention. That reference states that clustering in PEO/water systems is due to impurities in the water. This conclusion was reached after observing that the clusters disappeared upon filtering of the PEO/water solutions. We looked at this issue by dynamic light scattering and SANS and reached the following conclusions. Filtering (and even double distillation) of the water did not change the clustering observations reported here. Filtering of the PEO/water solutions broke the clusters. The clusters, however, were observed to re-form after hours to days (in agreement with ref 1). Our conclusion is, therefore, that clustering is not due to impurities in the water.

Acknowledgment. This work is based upon activities supported by the NSF under Agreement DMR-9986442. Certain products and equipment are mentioned by name only to clarify the experimental conditions used. It does not necessarily mean that they are the best for the purpose or that NIST endorses them. John Barker's help in taking USANS data is appreciated. Discussions with Charles Han and Theo van de Ven helped clarify certain aspects of this research.

References and Notes

(1) Polverari, M.; van de Ven, T. G. M. *J. Phys. Chem.* **1996**, *100*, 13687 and references therein.
(2) Caminati, W.; Moreschini, P.; Rossi, I.; Favero, P. G. *J. Am. Chem. Soc.* **1998**, *120*, 11144.
(3) Scheiner, S.; Cuma, M. *J. Am. Chem. Soc.* **1996**, *118*, 1511.
(4) Briscoe, B.; Luckham, P.; Zhu, S. *Macromolecules* **1996**, *29*, 6208.
(5) Sun, T.; King, H. E., Jr. *Macromolecules* **1998**, *31*, 6383.
(6) Horkay, F.; Hecht, A. M.; Geissler, E. *Macromolecules* **1998**, *31*, 8851.
(7) Zhou, C.; Hobbie, E.; Bauer, B. J.; Han, C. *J. Polym. Sci., Polym. Phys. Ed.* **1998**, *36*, 2745.
(8) Kahlweit, M.; Strey, R. *Angew. Chem., Int. Ed. Engl.* **1985**, *24*, 654. See the phase diagram in Figure 7 in this paper.
(9) Malcom, G. N.; Rowlinson, J. S. *Trans. Faraday Soc.* **1953**, *53*, 921.
(10) Devanand, K.; Selser, J. C. *Nature (London)* **1990**, *343*, 739.

MA011657N